Glucagon-like peptide-1 strengthens the barrier integrity in primary cultures of rat brain endothelial cells under basal and hyperglycemia conditions

Shuji Fukuda [a], Shinsuke Nakagawa [b, *], Rie Tatsumi [b], Yoichi Morofuji [a], Tomonori Takeshita [a], Kentaro Hayashi [a], Kunihiko Tanaka [c], Takayuki Matsuo [a], Masami Niwa [d, 1]

[a] *Department of Neurosurgery, Nagasaki University Graduate School of Biomedical Sciences, 1-7-1 Sakamoto, Nagasaki 852-8501, Japan*

[b] *Department of Medical Pharmacology, Nagasaki University Graduate School of Biomedical Sciences, 1-12-4 Sakamoto, Nagasaki 852-8523, Japan*

[c] *Advanced Medical Education Support Center, Nagasaki University School of Medicine, 1-12-4 Sakamoto, Nagasaki 852-8523, Japan*

[d] *BBB Laboratory, PharmaCo-Cell Company, Ltd., Nagasaki, 1-43 Dejima, Nagasaki 850-0862, Japan*

[1] *Professor emeritus at Nagasaki University*

* Corresponding author: S. Nakagawa; Fax: +81-95-819-7044

E-mail: shin3@nagasaki-u.ac.jp

Abstract

The objective of the present study was to determine the effects of glucagon-like peptide-1 (GLP-1) on barrier functions and to assess the underlying mechanism using an in vitro blood-brain barrier (BBB) model comprised of a primary culture of rat brain capillary endothelial cells (RBECs). GLP-1 increased transendothelial electrical resistance and decreased the permeability of sodium fluorescein in RBECs in a dose- and time-dependent manner. The effects on these barrier functions were significantly reduced in the presence of the GLP-1 receptor antagonist exendin-3 (9-39) and the protein kinase A (PKA) inhibitor H-89. Western blot analysis showed that GLP-1 increased the amount of occludin and claudin-5. GLP-1 analogs are approved for treatment of type 2 diabetes mellitus, and thus, we examined the effects of GLP-1 on hyperglycemia-induced BBB damage. GLP-1 inhibited the increase in production of reactive oxygen species under hyperglycemia conditions and improved the BBB integrity induced by hyperglycemia. As GLP-1 stabilized the integrity of the BBB, probably via cAMP/PKA signaling, the possibility that GLP-1 acts as a BBB-protective drug should be considered.

Keywords blood-brain barrier; glucagon-like peptide 1; cAMP/PKA signaling; tight junctions; hyperglycemia

Introduction

The blood-brain barrier (BBB) provides ionic homeostasis and nutrients that are necessary for the proper functioning of the central nervous system (CNS) and protects neurons from xenobiotics, blood-borne toxic substances, and stroke insults, as the barrier regulates levels of neuroactive mediators (Abbott, 2002; Zlokovic, 2008). In the BBB, tight junctions (TJs) are composed of cell-cell adhesion molecules and membrane proteins such as claudin, occludin, and zonula occludens (ZO-1). TJs are located between the brain capillary endothelial cells and restrict the paracellular diffusion of water-soluble substances from the blood into the brain, thus protecting neurons, an essential function of the BBB (Abbott, 2005; Deli et al. 2005). Thus, the presence of a complex network of TJs between endothelial cells plays a critical role in maintaining BBB properties (Miyoshi and Takai, 2005; Furuse and Tsukita, 2006; Van Itallie and Anderson 2006).

Glucagon-like peptide 1 (GLP-1) is an incretin hormone that is released into the bloodstream postprandially from the gut and binds to the GLP-1 receptor (GLP-1R) (Bell et al. 1983). Currently, GLP-1R agonists, such as exendin-4 (Ex-4), liraglutide, and lixisenatide, are approved for treatment of type 2 diabetes mellitus (Lovshin and Drucker, 2009; Wohlfart et al. 2013). A selective inhibitor of dipeptidylpeptidase-4 that functions as a long-acting agonist of GLP-1 is also clinically used worldwide for patients with type 2 diabetes mellitus (Drucker and Nauck, 2006; Darsalia et al. 2013; Yang et al. 2013). Diabetes is considered to be both a metabolic disease and a vascular disease because of its effects on macro- and microcirculation in numerous vascular beds, including cerebral vessels. Indeed, chronic hyperglycemia (HG) induces dysfunction of

vascular endothelial cells and is a key initial step in the pathology of diabetes. Several reports have shown that GLP-1 analogs has a beneficial effects on HG-induced endothelial dysfunctions (Sjöholm, 2009; Erdogdu et al. 2012;). The beneficial effects of GLP-1 are not limited to the treatment of diabetes but also provide significant neuroprotection in animal models of cerebral ischemia and Alzheimer's disease (During et al. 2003; Lee et al. 2011; Briyal et al. 2012; Sato et al. 2013; McClean and Hölscher, 2014). The underlying mechanisms of the neuroprotective effects of GLP-1 are not fully understood.

Dysfunction of brain capillary endothelial cells is considered to initiate the infiltration of toxic substrates and inflammatory cells into the brain, followed by neuronal damage. Thus, protection of BBB function likely mediates neuroprotection. Experimental evidence supports the benefits of protecting against BBB disruption by stimulating cyclic AMP (cAMP) signaling. In the last 20 years, studies have shown that intracellular elevation of cAMP in brain endothelial cells increases barrier integrity (Deli et al. 2005; Spindler et al. 2010). According to Maurice (2011), a molecular unit of cAMP/protein kinase A (PKA) and cAMP/exchange protein activated by cAMP 1 (Epac1) exerts barrier-stabilizing effects on endothelial cells through adherens junctions. In addition to the influence on adherens junctions, cAMP signaling also affects TJs of the BBB to increase the expression of claudin-5, a key protein of TJs, in a PKA-independent manner, and PKA activated by cAMP phosphorylates claudin-5 to strengthen barrier tightness (Ishizaki et al. 2003). Thus, cAMP signaling in brain endothelial cells is pertinent to the protection of the BBB. GLP-1 has various physiological effects via its specific receptors (GLP-1R), which are G protein-coupled receptors. As stimulation of GLP-1R activates the adenylyl cyclase pathway, which

induces the elevation of intracellular cAMP levels, GLP-1 may strengthen BBB properties.

In the present study, we investigated the in vitro effect of GLP-1 on cultured rat brain microvessel endothelial cells (RBECs) to elucidate the physiological significance of GLP-1 on the BBB.

Materials and Methods

All reagents were purchased from Sigma, USA, unless otherwise indicated. Wistar rats were obtained from Japan SLC, Inc., Japan. All animals were treated in strict accordance with the National Institutes of Health Guide for the Care and Use of Laboratory Animals (NIH Publications No. 80-23) and approved by the Nagasaki University Animal Care.

Primary cultures of RBEC

Primary cultures of rat brain capillary endothelial cells (RBEC) were prepared from 3-week-old rats, as described previously (Nakagawa et al. 2007 and 2009). Meninges were carefully removed from the forebrain and gray matter was minced into small pieces of 1 mm^3 in ice-cold Dulbecco's modified Eagle's medium (DMEM), followed by dissociation with 25 up-and-down strokes using a 5-mL pipette in DMEM containing collagenase type 2 (1 mg/mL; Worthington Biochemical Corp., Lakewood, NJ, USA), 300 μL of DNase (15 μg/mL) and gentamycin (50 μg/mL), and digestion in a shaker for

1.5 h at 37°C. Cell pellets were separated by centrifugation in 20% bovine serum albumin (BSA)-DMEM (1,000 × g, 20 min). The microvessels obtained in the pellet were further digested with collagenase-dispase (1 mg/mL; Roche Applied Sciences, Rotkreuz, Switzerland) and DNase (6.7 μg/mL in DMEM for 45 min at 37°C). RBEC clusters were separated on a 33% continuous Percoll (Pharmacia, Uppsala, Sweden) gradient, and were then collected and washed twice in DMEM before plating on 100-mm plastic dishes coated with collagen type IV (0.1 mg/mL) and fibronectin (0.1 mg/mL) (Day 0). RBEC cultures were maintained in DMEM/F12 supplemented with 10% fetal bovine plasma derived from serum (PDS) (Animal Technologies, Inc., Tyler, TX), basic fibroblast growth factor (bFGF, 1.5 ng/mL; Roche Applied Sciences), heparin (100 μg/mL), insulin (5 μg/mL), transferrin (5 μg/mL), sodium selenite (5 ng/mL) (insulin-transferrin-sodium selenite media supplement), gentamycin (50 μg/mL) and puromycin (4 μg/mL) (RBEC I medium) at 37°C under a humidified atmosphere of 5.0% CO_2/95% air for 2 days. Based on the findings of Perrière et al. (2005), in the first two days, cells were incubated in medium containing puromycin (4 μg/mL) in order to avoid contamination by pericytes. After 2 days, cells received new medium containing all the components of RBEC medium except for puromycin (RBEC II medium) (Day 2, Fig. 1). When cultures reached 80% confluence (Day 4), purified endothelial cells were passaged by brief treatment with trypsin (0.05% w/v)-EDTA (0.02% w/v) solution, and were used to construct the *in vitro* BBB model.

Construction of the in vitro BBB model

The day when endothelial cells were plated and models were established was defined as

day 4 *in vitro* (Fig. 1A). To construct an *in vitro* model of the BBB, endothelial cells (2.0×10^5 cells/cm^2) were seeded on the inside of inserts that were placed in the wells of 24-well culture plates. From day 5, BBB models were maintained in rat brain capillary endothelial cell (RBEC) medium II supplemented with 500 nM hydrocortisone. Under these conditions, *in vitro* BBB models were established within 3 days after setting of cells. Experiments with GLP-1 were carried out from Day 7 (Fig. 1).

Transendothelial electrical resistance (TEER)

To evaluate TJ function in RBEC, TEER were measured. TEER was measured using an EVOM resistance meter (World Precision Instruments, FL, USA). RBEC cultured on inserts in a 24-well plate were used to measure TEER. The resistance measurements of black filters (background resistance) were subtracted from filters with cells. The values are shown as $\Omega \times cm^2$, and data indicate the rate of change in TEER before and after treatment compared to control.

Transendothelial permeability

The flux of sodium fluorescein (Na-F), a small molecule permeability marker, across the endothelial monolayer was determined as previously described (Nakagawa et al. 2007). Cell culture inserts were transferred to 24-well plates containing 0.9 ml assay buffer (136 mM NaCl, 0.9 mM $CaCl_2$, 0.5 mM $MgCl_2$, 2.7 mM KCl, 1.5 mM KH_2PO_4, 10 mM NaH_2PO_4, 25 mM glucose, and 10 mM HEPES, pH 7.4) in the basolateral or lower compartments. In the inserts, the culture medium was replaced with 0.2 ml buffer

containing 10 μg/ml Na-F (MW: 376 Da). Then, 15 or 45 min after addition of Na-F, the inserts were transferred to new wells containing assay buffer. Na-F emission was measured at 535 nm (Wallac 1420 ARVO Multiabel Counter, Perkin Elmer, Waltham, MA, USA; excitation: 485 nm). The permeability of Na-F was used as an index of paracellular transport. Apparent permeability (Papp) was calculated using the following equation: $Papp = (dQ/dT)/(A \times C_0)$, where dQ/dT is the cumulative amount in the receiver compartment versus time, A is the surface of the filter, and C_0 is the initial concentration of the tracer in the luminal compartments.

GLP-1 treatment

GLP-1 (1-37) was purchased from Tocris Bioscience (Bristol, UK). One of two concentrations of GLP-1 (0.1, 1 μM) was added to the luminal sides of Millicell® inserts. At 0, 24, 48, and 72 h after GLP-1 addition to RBECs, barrier integrity was evaluated. The GLP-1R antagonist exendin-3 (9-39) amide (Ex-3 (9-39); 200 nM, Tocris Bioscience) and the PKA inhibitor H-89 (10 μM) were added 15 min prior to addition of GLP-1.

Western blot analysis

Cells were harvested by scraping in radioimmunoprecipitation assay buffer (RIPA; Santa Cruz Biotechnology, Santa Cruz, Dallas, TX, USA). Lysates were centrifuged at 15,000 × *g* for 5 min at 4°C, supernatants were collected, and protein concentrations were determined with the BCA protein assay reagent (Pierce, Rockford, IL, USA). An

equal amount of protein for each sample was separated on a 4–15% TGX (Tris-Glycine eXtended) gel (Bio-Rad, Hercules, CA, USA), transferred onto Hybond^{TM}-P (Amersham, Buckinghamshire, UK), and incubated with antibodies. Anti-claudin-5, anti-occludin, and anti-ZO-1 mouse monoclonal antibodies (Invitrogen Corporation, Carlsbad, CA, USA) were used at dilutions of 1:5,000. Anti-β-actin mouse monoclonal antibody (additional loading control) was used at a dilution of 1:10,000 in 3% bovine serum albumin in phosphate-buffered saline. To visualize the immunoreactive bands, blots were incubated in SuperSignal West Femto Maximum Sensitivity Substrate SECL in accordance with the manufacturer's instructions (Pierce Biotechnology) and were detected using a FluorChem SP Imaging System (Alpha Innotech Corp., San Leandro, CA, USA).

Hyperglycemia (HG) treatment

Based on previous reports (Yan et al. 2012) and our preliminary examination, we used a concentration of 55 mM D-glucose for HG-induced BBB dysfunction. RBECs were exposed to 55 mM D-glucose (WAKO Pure Chemical Ltd., Osaka, Japan) with or without GLP-1 in RBEC II medium. After 48 h, cell viability, TEER, and transendothelial permeability were measured.

Cell viability

RBECs were seeded at a density of 5,000 cells per well into 96-well plates in culture medium. After exposure to HG for 48 h, the number of viable cells was determined

using the Cell Counting Kit 8 (Dojindo Co., Kumamoto, Japan) according to the manufacturer's instructions. The assay reagent is a tetrazolium compound (WST-8) that is reduced by live cells to a colored formazan product, the absorbance of which is measured at 450 nm.

Measurement of reactive oxygen species (ROS)

Intracellular ROS production was measured by evaluating oxidation of the cell-permeable fluorescent probe 5-(and-6)-chloromethyl-2',7'-dichlorodihydrofluorescein diacetate, acetyl ester (CM-H_2DCFDA, Invitrogen). RBECs (5,000/well) were seeded into 96-well plates. After reaching confluency, cells were washed twice with the assay buffer indicated in the permeability section. Cells were pre-incubated with 0.1 ml assay buffer containing 10 μM CM-H_2DCFDA and GLP-1 (0, 0.1 μM) for 1 h. After pre-incubation, cells were washed twice with assay buffer, and D-glucose (0, 55 mM) and GLP-1 (0, 0.1 μM) were added for 1 h. Fluorescein intensity derived from CM-H_2DCFDA was determined using a fluorescence multi-well plate reader (Ex(λ) 485 nm; Em(λ) 535 nm). Cellular protein was measured with the BCA protein assay kit, and the data were normalized to protein content.

Statistical Analysis

All data are expressed as the means ± standard error of the mean (SEM). Values were compared using analysis of variance followed by the Tukey-Kramer method. A p value of less than 0.05 was considered to be statistically significant.

Results

Effects of GLP-1 on barrier integrity in RBECs

TEER in our monolayer model of cultured RBECs was more than 120 Ω × cm^2 (the control value at 0 min was 127.1 ± 3.8 Ω × cm^2, n = 8, Fig. 2a). To examine whether GLP-1 affected the barrier integrity of RBECs, TEER and paracellular permeability of Na-F (MW 376) were measured. Treatment with 0.1 and 1 μM GLP-1 for 72 h significantly elevated TEER in RBECs to 118.7 ± 4.7% and 139.9 ± 4.2% of the control, respectively (Fig. 2a). GLP-1 also affected the paracellular permeability of Na-F, a small water-soluble marker, across the RBEC monolayer at 72 h after treatment with GLP-1. Treatment with 0.1 and 1 μM GLP-1 significantly decreased the permeability of Na-F in RBECs to 67.7 ± 5.3% and 56.8 ± 2.2% of the control, respectively (Papp control value was 9.1 ± 1.7 × 10^{-6} cm/s) (Fig. 2b). Thus, GLP-1 strengthened the BBB properties of RBECs.

Effect of GLP-1 on TJ proteins in RBECs

To investigate whether regulation of barrier functions is induced by GLP-1 in RBECs, changes in TJ protein levels in GLP-1-treated RBECs were investigated with western blot analysis. As shown in Fig. 3, no differences were found in ZO-1 protein levels between control and GLP-1-treated RBECs. In contrast, GLP-1 significantly increased the protein levels of occludin and claudin-5 (Fig. 3). Treatment with 1 μM GLP-1

significantly increased the protein level of occludin and claudin-5 in RBECs to 149.0 ± 17.5% and 179.3 ± 21.2% of the control, respectively.

Effect of the GLP-1R antagonist Exendin-3 (9-39) amide and the effect of the PKA inhibitor H-89 on GLP-1-induced enhancement of TJ functions in RBECs

To examine whether the effect of GLP-1 on barrier functions is related to GLP-1R, we used the GLP-1R antagonist Exendin-3 (9-39) amide (Ex-3 (9-39)) in RBECs. Ex-3 (9-39) alone did not affect TEER. However, Ex-3 (9-39) prevented the increase in TEER that was induced by GLP-1 treatment for 48 h (Fig. 4a). Several reports have shown that stimulation of GLP-1R induces an increase in intracellular cAMP levels (Li et al. 2015; Donnelly, 2012). An elevation in cAMP induces the activation of PKA, a major target of cAMP. To examine whether the effect of GLP-1 on barrier functions is related to the cAMP/PKA pathway, we examined the effect of the PKA inhibitor H-89 in RBECs. The effect of GLP-1 on the increase in TEER was prevented by adding the PKA inhibitor H-89 for 48 h (Fig. 4b). Thus, GLP-1 strengthened the barrier properties via the cAMP/PKA pathway.

Effects of GLP-1 on barrier integrity in RBECs under hyperglycemia

GLP-1R agonists are approved for treatment of type 2 diabetes mellitus. Chronic hyperglycemia (HG) induces dysfunction of vascular endothelial cells and is a key initial step in the pathology of diabetes. To examine whether GLP-1 improves HG-induced BBB dysfunction, we examined the effects of GLP-1 on RBECs under HG

conditions. As oxidative stress is a factor that induces cellular damage under HG, we analyzed the effects of GLP-1 on cell viability and production of ROS. We found no significant difference in cell viability as a result of normoglycemia (NG) or HG for 48 h (Fig. 5a). ROS production was significantly higher in HG than NG (132.3 ± 4.5 vs. 100 ± 5.0%; $p < 0.05$), and GLP-1 (0.1, 1 μM) reduced the ROS production induced by HG (Fig. 5b). Finally, we investigated the effects of GLP-1 against HG-induced BBB damage by measuring TEER and Na-F permeability. Treatment with D-glucose (55 mM) significantly decreased TEER and increased Na-F permeability compared with the control at 48 h. GLP-1 (0.1 μM) significantly blocked the HG-induced reduction in TEER and the HG-induced increase in Na-F permeability (Fig. 5c, d).

Discussion

The BBB plays an important role as an interface between the blood and brain tissues. As disruption of the BBB evokes brain edema formation and neuronal damage, strengthening of the integrity of the BBB plays a crucial role in protection against development of neurological disorders. In the present study, GLP-1 strengthened the barrier integrity in primary cultures of RBECs and increased the expression of occludin and claudin-5 via cAMP/PKA pathway. These findings imply that GLP-1 may act as a BBB protective drug for CNS disorders.

Several studies have demonstrated the therapeutic effect of GLP-1 analogs in animal models of Alzheimer's disease and stroke (Briyal et al. 2012; Sato et al. 2013; McClean and Hölscher, 2014). GLP-1 analogs reduce endogenous levels of β-amyloid

in the brain, prevent impairment in learning new spatial tasks, decrease synaptic loss, and reduce plaque load (McClean et al. 2011; Perry et al. 2003). Briyal et al. (2012) demonstrated that repeated administration of Ex-4 significantly improves infarct volume, neurological deficits, and oxidative stress parameters in ischemic rats. Ex-4 also protects against ischemia-induced neuronal death, possibly by increasing GLP-1R expression to prevent transient cerebral ischemic damage (Lee et al. 2011). Another study showed that liraglutide reduces infarct volume and oxidative stress parameters and increases cortical vascular endothelial growth factor (Sato et al. 2013). These findings led to the suggestion that stimulation of GLP-1R could be valuable for treating neurological disorders and preventing further damage. Although several studies have examined the neuroprotective effect of GLP-1 analogs in animal models, no report has examined the direct effects of GLP-1 on the barrier function of RBECs in normal culture conditions.

GLP-1R is a G protein-coupled receptor and a well-known direct activator of adenylate cyclase. The two main signaling axes downstream of cAMP are activation of PKA and engagement of Epac and its effector GTPase Rac1 (Dodge-Kafka et al. 2005). In the present study, we observed that GLP-1 increased TEER in RBECs in a dose- and time-dependent manner and reduced the permeability of Na-F. This effect was inhibited by the GLP-1R antagonist Ex-3 (9-39) and the PKA inhibitor H-89, suggesting that the binding of GLP-1 to GLP-1R activates the cAMP/PKA pathway to alter the barrier function in RBECs. Li et al. (2015) demonstrated that Ex-4 enhances endothelial barrier function via PKA- and Epac-1-dependent Rac1 activation. Our findings indicate that GLP-1 strengthens the barrier integrity via the cAMP/PKA pathway in RBECs.

To examine if the effect of GLP-1 on TEER is related to expression of TJ proteins,

we analyzed the expression of TJ proteins with western blotting. Claudin-5 and occludin are the main component proteins of TJ strands and play crucial roles in TJ function (Furuse and Tsukita, 2006; Abbott et al. 2010). Although no clear changes in ZO-1 were observed with western blotting after GLP-1 treatment, GLP-1 increased the protein level of occludin and claudin-5. cAMP signaling increases the expression of claudin-5 via both PKA-dependent and -independent pathways (Ishizaki et al. 2003; Beese et al. 2010). In addition, a cAMP analog increases the expression of occludin in a PKA-dependent manner and decreases the levels of intracellular cAMP, which decreases PKA activity and occludin protein expression (Beese et al. 2010; Li et al. 2011). Taken together with these reports, the effects of GLP-1 on barrier functions appear to be mainly associated with increased expression of claudin-5 and occludin via the cAMP/PKA pathway.

Diabetes is considered to be both a metabolic disease and a vascular disease because of its effects on macro- and microcirculation in numerous vascular beds, including cerebral vessels. Generally, diabetes or chronic HG contributes to proliferation of vascular smooth muscle cells, degeneration of endothelial cells and pericytes, thickening of the capillary basement membrane, and increased aggregation and adhesion of platelets to the endothelium (Ergul et al. 2009). Shao and Bayraktutan (2013) reported that HG compromises the structural and functional capacities of an in vitro model of the human cerebral barrier. Vannucci et al. (2001) and Tureyen et al. (2011) have reported that a type-2 diabetes mouse model that was subjected to focal ischemia shows significantly higher mortality, larger infarcts, increased cerebral edema, and worse neurological status compared to nondiabetic animals. Therefore, we investigated the effects of GLP-1 against HG-induced BBB damage in RBECs. HG

plays a critical role in the progress of diabetic angiopathy. Indeed, chronic exposure to HG damages cells. Although several molecular mechanisms appear to be related to HG-induced endothelial dysfunction, substantial evidence shows that HG increases the production of ROS. Hence, we examined the effects of GLP-1 on cell viability and ROS production. Although GLP-1 and HG did not influence cell viability, ROS production was significantly higher in HG than NG, and GLP-1 reduced the ROS production induced by HG. Recent reports indicate that GLP-1 can protect against ROS-induced cell stress through PKA activation or AMP-activated protein kinase activation (Oeseburg et al. 2010; Balteau et al. 2014). Although further studies are needed, our finding that GLP-1 protected brain capillary endothelial cells from HG-induced oxidative stress may be related to these pathways.

Finally, we examined the effects of GLP-1 on BBB properties following HG for 48 h. GLP-1 significantly blocked the HG-induced reduction in TEER and the HG-induced elevation in Na-F permeability. In agreement with our observation under normal culture conditions (Fig. 2a), 0.1 μM GLP-1 did not affect the BBB function under 48-h NG conditions. Considering that acceleration of ROS production induces hyperpermeability (Boueiz and Hassoun, 2009; Pun et al. 2009), the protective effects of GLP-1 on BBB function under HG appear to be related to reduction of ROS production. Although further studies are needed to determine whether these signaling pathways are associated with regulation of barrier function in GLP-1-treated RBECs under HG, this finding suggests that GLP-1 may act as a BBB-protective drug for diabetic cerebral vessel disease.

In summary, GLP-1 strengthened the barrier integrity in primary cultures of RBECs and increased the expression of occludin and claudin-5 via the cAMP/PKA pathway.

Our present study suggests the therapeutic importance of GLP-1 for protecting the BBB in conditions of diabetic angiopathy and other types of CNS damage.

Acknowledgment

This work was supported in part by a Grant-in-Aid for Young Scientists (B) (24790258) from the Japan Society for the Promotion of Science (JSPS). We would like to thank Keisuke Toyoda, Gohei So for their critical reviews of the manuscript and helpful professional guidance.

Conflict of interest

All authors have no competing interests.

Reference

Abbott NJ (2002) Astrocyte-endothelial interactions and blood-brain barrier permeability. J Anat 200:629–638.

Abbott NJ (2005) Dynamics of CNS barriers: Evolution, differentiation, and modulation. Cell Mol Neurobiol 25:5–23

Abbott NJ, Patabendige AA, Dolman DE, Yusof SR, Begley DJ (2010) Structure and function of the blood-brain barrier. Neurobiol Dis 37:13-25

Balteau M, Van Steenbergen A, Timmermans AD, et al. (2014) AMPK activation by glucagon-like peptide-1 prevents NADPH oxidase activation induced by

hyperglycemia in adult cardiomyocytes. Am J Physiol Heart Circ Physiol 307:H1120-133

Beese M, Wyss K, Haubitz M, Kirsch T (2010) Effect of cAMP derivates on assembly and maintenance of tight junctions in human umbilical vein endothelial cells. BMC Cell Biol 11:68 doi: 10.1186/1471-2121-11-68.

Bell GI, Sanchez-Pescador R, Laybourn PJ, Najarian RC (1983) Exon duplication and divergence in the human preproglucagon gene. Nature 304:368-371

Boueiz A, Hassoun PM (2009) Regulation of endothelial barrier function by reactive oxygen and nitrogen species. Microvasc Res 77:26-34

Briyal S, Gulati K, Gulati A (2012) Repeated administration of exendin-4 reduces focal cerebral ischemia-induced infarction in rats. Brain Res 1427:23-34

Darsalia V, Ortsäter H, Olverling A, et al. (2013) The DPP-4 inhibitor linagliptin counteracts stroke in the normal and diabetic mouse brain: A comparison with glimepiride. Diabetes 62:1289-1296

Deli MA, Ábrahám CS, Kataoka Y, Niwa M (2005) Permeability studies on in vitro blood-brain barrier models: Physiology, pathology, and pharmacology. Cell Mol Neurobiol 25:59–127

Dodge-Kafka KL, Soughayer J, Pare GC, et al. (2005) The protein kinase A anchoring protein mAKAP coordinates two integrated cAMP effector pathways. Nature 437:574-578

Donnelly D (2012) The structure and function of the glucagon-like peptide-1 receptor and its ligands. Br J Pharmacol 166:27-41

Drucker DJ, Nauck MA (2006) The incretin system: glucagon-like peptide-1 receptor agonists and dipeptidyl peptidase-4 inhibitors in type 2 diabetes. Lancet 368:1696-1705

During MJ, Cao L, Zuzga DS, et al. (2003) Glucagon-like peptide-1 receptor is involved in learning and neuroprotection. Nat Med 9:1173-1179

Erdogdu Ö, Eriksson L, Nyström T, Sjöholm Å, Zhang Q (2012) Exendin-4 restores glucolipotoxicity-induced gene expression in human coronary artery endothelial cells. Biochem Biophys Res Commun 419:790-795

Ergul A, Li W, Elgebaly MM, Bruno A, Fagan SC (2009) Hyperglycemia, diabetes and stroke: focus on the cerebrovasculature. Vasc Pharmacol 51:44-49

Furuse M, Tsukita S (2006) Claudins in occluding junctions of humans and flies. Trends Cell Biol 16:181-188

Ishizaki T, Chiba H, Kojima T, et al. (2003) Cyclic AMP induces phosphorylation of claudin-5 immunoprecipitates and expression of claudin-5 gene in blood-brain-barrier endothelial cells via protein kinase A-dependent and -independent pathways. Exp Cell Res 290:275-288

Lee CH, Yan B, Yoo KY, et al. (2011) Ischemia-induced changes in glucagon-like peptide-1 receptor and neuroprotective effect of its agonist, exendin-4, in experimental transient cerebral ischemia. J Neurosci Res 89:1103-1113

Li AQ, Zhao L, Zhou TF, Zhang MQ, Qin XM (2015) Exendin-4 promotes endothelial barrier enhancement via PKA- and Epac1-dependent Rac1 activation. Am J Physiol Cell Physiol 308:C164-175

Li Z, Liu YH, Xue YX, Xie H, Liu LB (2011) Role of ATP synthase alpha subunit in low-dose endothelial monocyte-activating polypeptide-II-induced opening of the blood-tumor barrier. J Neurol Sci 300:52-58

Lovshin JA, Drucker DJ (2009) Incretin-based therapies for type 2 diabetes mellitus. Nat Rev Endocrinol 5:262-269

Maurice DH (2011) Subcellular signaling in the endothelium: Cyclic nucleotides take their place. Curr Opin Pharmacol 11:656-664

McClean PL, Parthsarathy V, Faivre E, Hölscher C (2011) The diabetes drug liraglutide prevents degenerative processes in a mouse model of Alzheimer's disease. J Neurosci 31:6587-6594

McClean PL, Hölscher C (2014) Liraglutide can reverse memory impairment, synaptic loss and reduce plaque load in aged APP/PS1 mice, a model of Alzheimer's disease. Neuropharmacology 76:57-67

Miyoshi J, Takai Y (2005) Molecular perspective on tight-junction assembly and epithelial polarity. Adv Drug Deliv Rev 57:815-855

Nakagawa S, Deli MA, Nakao S, et al. (2007) Pericytes from brain microvessels strengthen the barrier integrity in primary cultures of rat brain endothelial cells. Cell Mol Neurobiol 27:687-694

Nakagawa S, Deli MA, Kawaguchi H, et al. (2009) A new blood-brain barrier model using primary rat brain endothelial cells, pericytes and astrocytes. Neurochem Int 54:253–263

Oeseburg H, de Boer RA, Buikema H, van der Harst P, van Gilst WH, Silljé HH (2010) Glucagon-like peptide 1 prevents reactive oxygen species-induced endothelial cell senescence through the activation of protein kinase A. Arterioscler Thromb Vasc Biol 30:1407-1414

Perriere N, Demeuse P, Garcia E, et al. (2005) Puromycin-based purification of rat brain capillary endothelial cell cultures. Effect on the expression of blood-brain barrier-specific properties. J Neurochem 93:279-289

Perry T, Lahiri, DK Sambamurti, K et al. (2003) Glucagon-like peptide-1 decreases endogenous amyloid-beta peptide (Abeta) levels and protects hippocampal neurons from death induced by Abeta and iron. J Neurosci Res 72:603-612

Pun PB, Lu J, Moochhala S (2009) Involvement of ROS in BBB dysfunction. Free Radic Res 43:348-364

Sato K, Kameda M, Yasuhara T, et al. (2013) Neuroprotective effects of liraglutide for stroke model of rats. Int J Mol Sci 14:21513-21524

Shao B, Bayraktutan U (2013) Hyperglycaemia promotes cerebral barrier dysfunction through activation of protein kinase C-beta. Diabetes Obes Metab 15:993–999

Spindler V, Schlegel N, Waschke J (2010) Role of GTPases in control of microvascular permeability. Cardiovasc Res 87:243-253

Sjöholm A (2009) Impact of glucagon-like peptide-1 on endothelial function. Diabetes Obes Metab Suppl 3:19-25

Tureyen K, Bowen K, Liang J, Dempsey RJ, Vemuganti R (2011) Exacerbated brain damage, edema and inflammation in type-2 diabetic mice subjected to focal ischemia. J Neurochem 116:499-507

Van Itallie CM, Anderson JM (2006) Claudins and epithelial paracellular transport. Annu Rev Physiol 68:403-429

Vannucci SJ, Willing LB, Goto S, et al. (2001) Experimental stroke in the female diabetic, db/db, mouse. J Cereb Blood Flow Metab 21:52–60

Wohlfart P, Linz W, Hübschle T, et al. (2013) Cardioprotective effects of lixisenatide in rat myocardial ischemia-reperfusion injury studies. J Transl Med 11:84 doi: 10.1186/1479-5876-11-84

Yan J, Zhang Z, Shi H (2012) HIF-1 is involved in high glucose-induced paracellular permeability of brain endothelial cells. Cell Mol Life Sci 69:115-128

Yang D, Nakajo Y, Iihara K, Kataoka H, Yanamoto H (2013) Alogliptin, a dipeptidylpeptidase-4 inhibitor, for patients with diabetes mellitus type 2, induces tolerance to focal cerebral ischemia in non-diabetic, normal mice. Brain Res 1517:104-113

Zlokovic BV (2008) The Blood-Brain Barrier in Health and Chronic Neurodegenerative Disorders. Neuron 57:178–201

Legends for Figures

Fig. 1 Schematic drawing of the experiment with primary cultures of rat brain capillary endothelial cells (RBECs). RBECs were isolated 4 days before establishment of the in vitro blood-brain barrier (BBB) model. To purify cultures, cells were maintained in the presence of puromycin for 2 days. On day 4, RBECs were seeded in the luminal compartment of the inserts and positioned in the 24-well plates. From day 5, RBECs were grown in culture medium containing 500 nM hydrocortisone. Glucagon-like peptide 1 (GLP-1) was added on day 7, and transendothelial electrical resistance (TEER) was monitored on days 7-10. On day 10, the permeability assay was performed.

Fig. 2 Effects of GLP-1 on barrier integrity in RBECs. The barrier integrity was assessed by measuring TEER and the transendothelial permeability (Papp) of the paracellular transport marker sodium fluorescein (Na-F) across endothelial monolayers. **a** GLP-1 increased TEER in RBECs in a dose- and time-dependent manner. Confluent RBEC cultures were exposed to GLP-1 at concentrations of 0.1 and 1 μM for up to 72 h. Significantly higher TEER was detected in RBECs treated with 1 μM GLP-1 for 48 and 72 h. The control value of TEER in RBECs was 127.1 ± 3.8 Ω × cm^2 at 0 h. All data are presented as the means ± SEM (n = 8). *p < 0.05 and **p < 0.01, significant difference from control. **b** GLP-1 reduced Na-F Papp in RBECs. The cells were treated with increasing concentrations of GLP-1 for 72 h. Significantly lower Papp values for Na-F were detected in RBECs treated with 0.1 μM and 1 μM GLP-1. Papp values are expressed as a percent of the control value. The control value of Papp for Na-F was 9.1 ± 1.7 × 10^{-6} cm/s. All data are presented as the means ± SEM (n = 8). **p < 0.01,

significant difference from control.

Fig. 3 Effect of GLP-1 on the expression of TJ proteins in RBECs. **a** Western blot analyses of ZO-1, claudin-5, and occludin were performed after 48 h of treatment of RBECs with 1 μM GLP-1. Fig. 3a shows representative images. **b** The level of expression of each protein was normalized to the corresponding internal control (β-actin). GLP-1 increased the expression of occludin and claudin-5 in RBECs. All data are presented as the means ± SEM ($n = 5$). $^{**}p < 0.01$, significant difference from control.

Fig. 4 Effect of the GLP-1R antagonist exendin-3 (Ex-3) (9-39) and the effect of the protein kinase A (PKA) inhibitor H-89 on GLP-1-induced enhancement of TJ functions in RBECs. **a** TEER was significantly elevated in RBECs treated with 1 μM GLP-1 for 48 h. $^{**}p < 0.01$, significant difference from control (open column). Ex-3 (9-39) completely blocked the GLP-1-induced increase in TEER (hatched column). $^{\#}p < 0.05$, significant difference from GLP-1 alone. The TEER values are expressed as a percent of the control value. The control values for TEER in RBECs at 48 h were 174.7 ± 25.7 Ω × cm^2. All data are presented as the means ± SEM ($n = 9$). **b** TEER was significantly elevated in RBECs treated with 1 μM GLP-1 for 48 h. $^{**}p < 0.01$, significant difference from control. H-89 (10 μM) completely blocked the GLP-1-induced increase in TEER. $^{\#}p < 0.01$, significant difference from GLP-1 alone. The TEER values are expressed as a percent of the control value. The control value of TEER in RBECs was 125.6 ± 24.7 Ω × cm^2. All data are presented as the means ± SEM ($n = 13$).

Fig. 5 Effects of GLP-1 on RBECs under hyperglycemia (HG). **a** Cell viability under HG. No significant difference in the cell number was observed between control and HG, and GLP-1 did not affect the cell viability. All data are presented as the means ± SEM (n = 5). **b** Significantly higher production of ROS was detected in RBECs treated with D-glucose (55 mM). GLP-1 (0.1, 1 μM) reduced the ROS production induced by HG. All data are presented as the means ± SEM (n = 5). The barrier integrity was assessed with TEER and the transendothelial permeability (Papp) of the paracellular transport marker sodium fluorescein (Na-F) across endothelial monolayers. **c** TEER was significantly reduced in RBECs treated with HG for 48 h. GLP-1 significantly blocked the HG-induced reduction in TEER. All data are presented as the means ± SEM (n = 8). **d** Na-F permeability was significantly elevated in RBECs treated with HG for 48 h. GLP-1 significantly blocked the HG-induced elevation in Na-F permeability. The control value of Papp for Na-F was $5.5 \pm 1.9 \times 10^{-6}$ cm/s. All data are presented as the means ± SEM (n = 4). **a-d** The values are expressed as a percent of normoglycemia control value. *p < 0.05 and **p < 0.01, significant difference from normoglycemia control. $^{\#}p$ < 0.05, significant difference from the HG control group.

Fig. 1

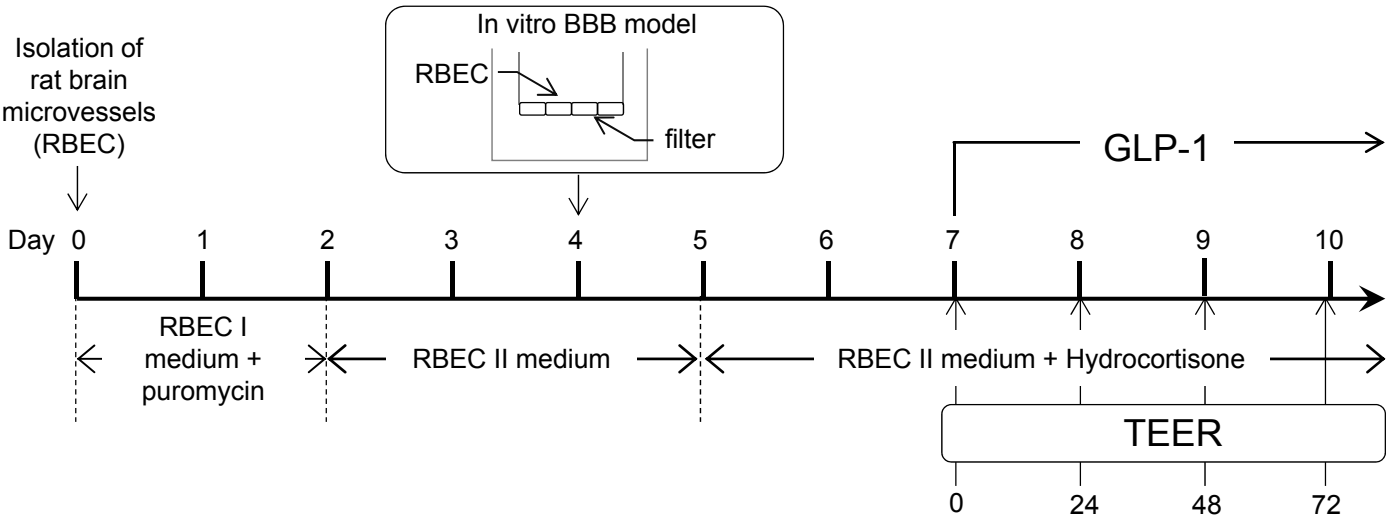
Isolation of rat brain microvessels (RBEC)
In vitro BBB model
RBEC
filter
GLP-1
Day 0 1 2 3 4 5 6 7 8 9 10
RBEC I medium + puromycin
RBEC II medium
RBEC II medium + Hydrocortisone
TEER
0 24 48 72

Fig. 2

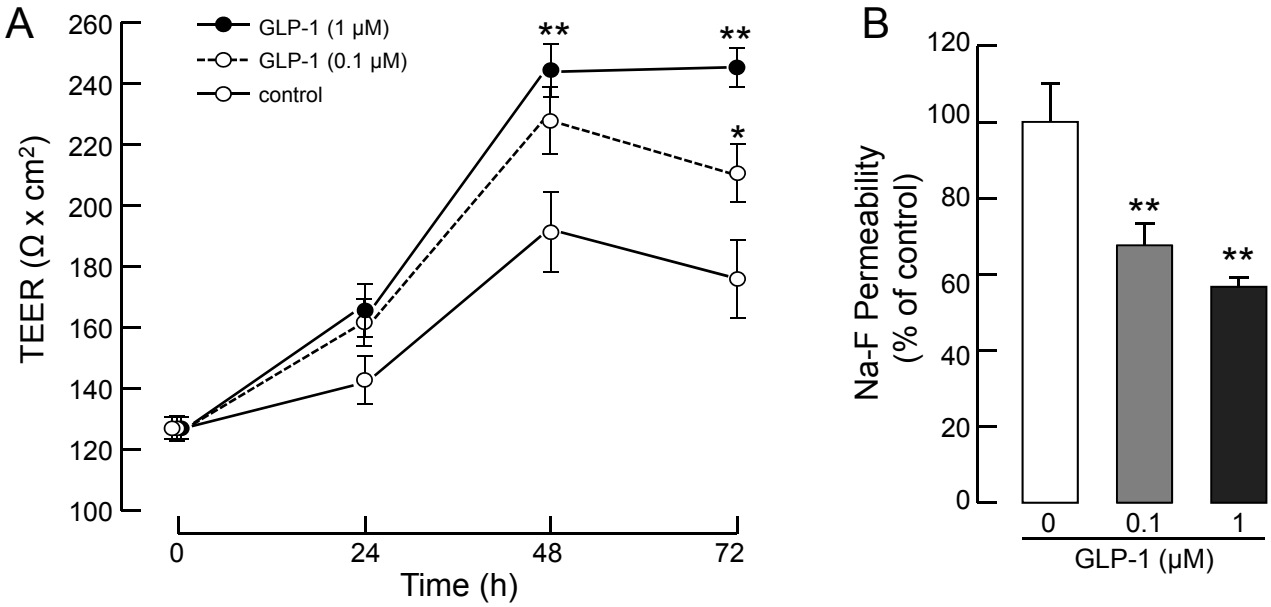
A
GLP-1 (1 μM)
GLP-1 (0.1 μM)
control
TEER (Ω x cm²)
260
240
220
200
180
160
140
120
100
**
**
*
0
24
48
72
Time (h)
B
Na-F Permeability
(% of control)
120
100
80
60
40
20
0
**
**
0
0.1
1
GLP-1 (μM)

Fig. 3

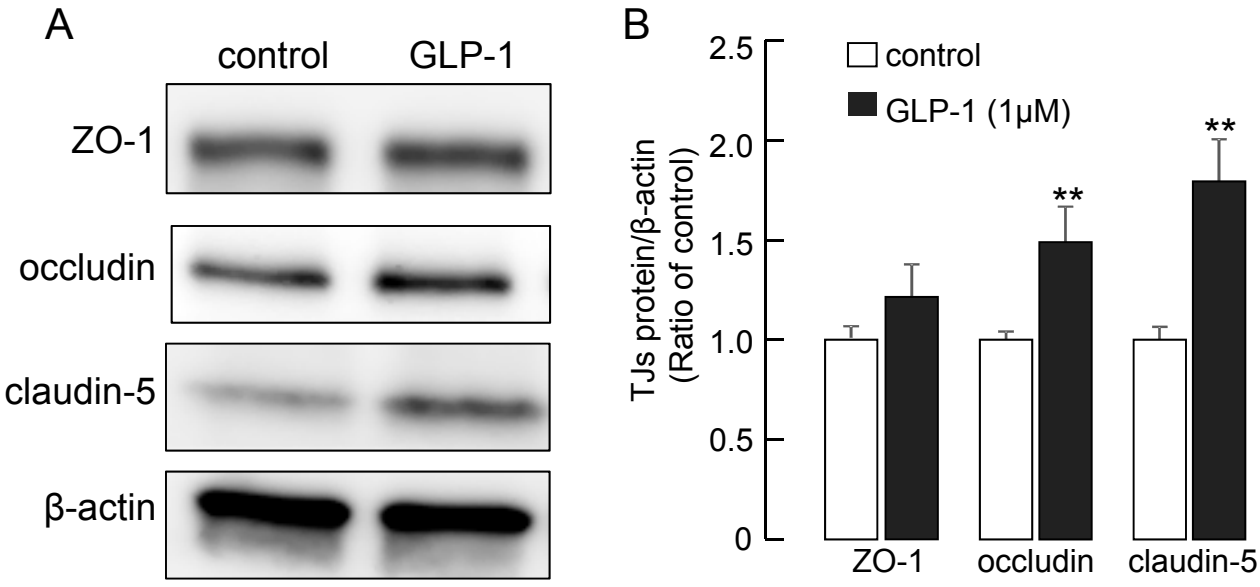
A
control
GLP-1
ZO-1
occludin
claudin-5
β-actin
B
control
GLP-1 (1μM)
TJs protein/β-actin
(Ratio of control)
2.5
2.0
1.5
1.0
0.5
0
**
**
ZO-1
occludin
claudin-5

Fig. 4

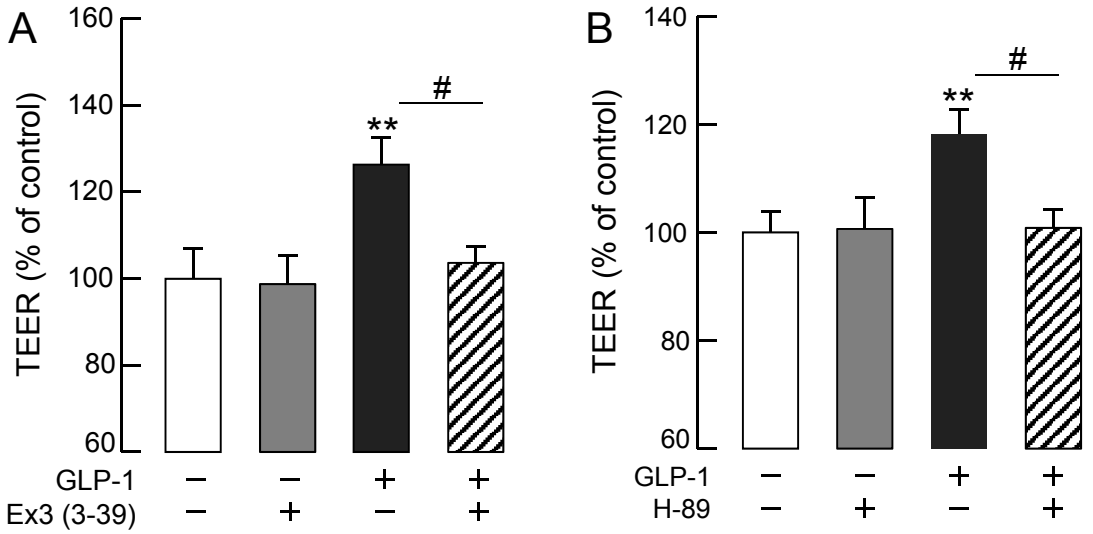
A
TEER (% of control)
160
140
120
100
80
60
**
#
GLP-1 − − + +
Ex3 (3-39) − + − +
B
TEER (% of control)
140
120
100
80
60
**
#
GLP-1 − − + +
H-89 − + − +

Fig. 5

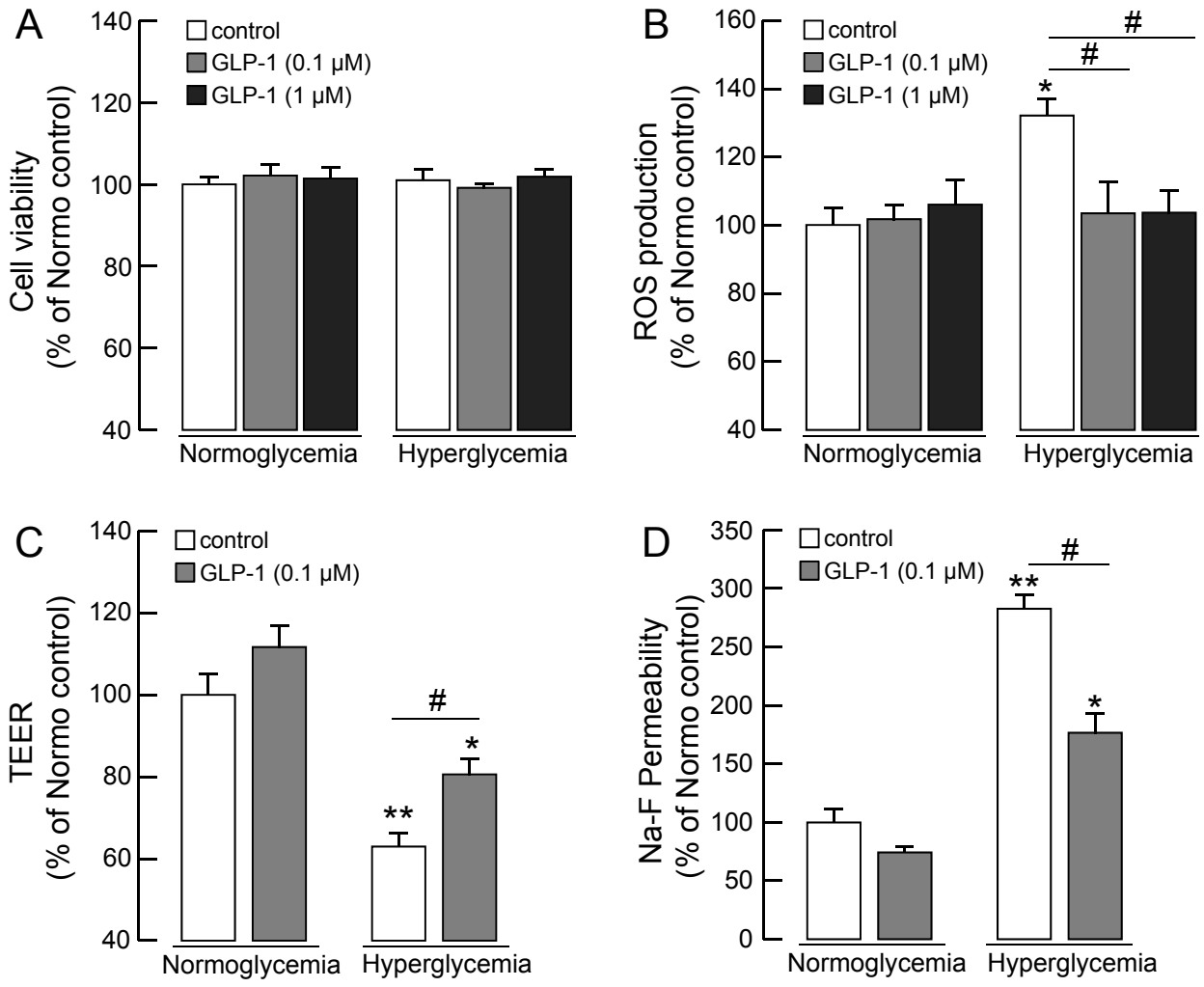
A
Cell viability
(% of Normo control)
control
GLP-1 (0.1 μM)
GLP-1 (1 μM)
Normoglycemia
Hyperglycemia
B
ROS production
(% of Normo control)
C
TEER
(% of Normo control)
D
Na-F Permeability
(% of Normo control)